

## Copper/reduced graphene oxide nanocomposite for high performance photocatalytic methylene blue dye degradation

Belete Asefa Aragaw<sup>1,\*</sup> and Atsedemariam Dagnaw<sup>1</sup>

<sup>1</sup>Bahir Dar University, Department of Chemistry, PO Box 79, Bahir Dar, Ethiopia

### Abstract

Copper nanoparticles deposited on reduced graphene oxide (RGO) have been investigated for various applications. In many of these reports RGO is used as a support and electron collector and not as a light absorber. However, Cu nanoparticle decorated over the surface of semiconducting RGO as a light absorber has not been investigated for its photocatalytic organic dye degradation activity. Here, we deposited Cu nanoparticle on RGO sheet by insitu photoreduction method. The Cu/RGO nanocomposite photocatalyst material is characterized by UV-Visible spectroscopy, FT-IR and X-ray powder diffraction and its photodegradation activity towards model organic dye was investigated. Based on our results, it was found that the photocatalytic degradation efficiency of GO, RGO and Cu/RGO nanocomposites were 63%, 68% and 94%, respectively under light irradiation at pH~7 in 50 min. The high photocatalytic performance of Cu/RGO nanocomposite is due to the catalytic effect of Cu. The Cu nanoparticle is a good photoelectron acceptor that traps the photoelectron and reduces the recombination rate of photoelectron-hole pairs. We believe that our finding would be widely applicable to the graphene oxide based composites with metal or metal oxide nanoparticles to develop a cost effective technique for environmental protection.

**Keywords:** Cu nanoparticle, Nanocomposites, Reduced graphene oxide, Organic dye degradation, Photocatalysts  
DOI: <https://dx.doi.org/10.4314/ejst.v12i2.2>

---

\*Corresponding author: [beliyeed@gmail.com](mailto:beliyeed@gmail.com), Tel: +251-911-979-678

## INTRODUCTION

Color removal from textile and paper industries effluents remains a serious challenge and the cause of serious effects in water bodies as it reduces light penetration and hence death of aquatic life. Therefore, the efficient treatment of waste waters has become of immediate importance among the scientific community around the globe as there is a growing need to come out with the state of the art technologies that are capable to solve the problems. Ideally an effective waste water treatment is to mineralize completely all the toxic contaminants in waste water without leaving any hazardous residues. In addition the waste water treatment process should be cost effective and feasible for large scale applications. These techniques include coagulation and sedimentation in which sediments again create disposal problems. Other techniques include the use of constructed wetlands but are expensive to construct, require more space and minimal chances of success as the ecological conditions may not favor particular plant species that are known to remove heavy metals. Photocatalytic dye degradation process is the most promising technology of advanced oxidation process for mineralizing organic pollutants (Tanaka *et al.*, 2000; da Silva *et al.*, 2003; Mahmoodi *et al.*, 2017). Several semiconducting metal oxide materials including TiO<sub>2</sub> (Akbal, 2005; Barka *et al.*, 2010), ZnO (Rajamanickam *et al.*, 2016), Fe<sub>2</sub>O<sub>3</sub> (Zang *et al.*, 2010), WO<sub>3</sub> (Carcel *et al.*, 2011), CuO (Nezamzadeh-Ejhih *et al.*, 2010; Nezamzadeh-Ejhih *et al.*, 2013, 2014), and non-metallic oxide such as GO (Zhang *et al.*, 2010; Sun *et al.*, 2012) have been investigated for their good photocatalytic organic waste treatment activities. GO based photocatalyst materials have several advantages over the other materials because they are non-toxic, low cost of the precursor material and ease of synthesis from graphite powder. Because of these merits, GO based photocatalyst materials have been investigated in several applications including photocatalytic hydrogen production from water splitting (Yeh *et al.*, 2010; Yeh *et al.*, 2011; Jiang *et al.*, 2013), antimicrobial activity (Sun *et al.*, 2017; Liu *et al.*, 2019; Wei *et al.*, 2019), photocatalytic CO<sub>2</sub> to methanol conversion (Hsu *et al.*, 2013; Kumar *et al.*, 2015), and photodegradation of organic pollutant in waste water (Zhang *et al.*, 2010; Sun *et al.*, 2012). To decrease the larger band gap of GO, a controlled reduction can be introduced to make RGO. GO and RGO have been coupled with other semiconductors and metals to improve its photocatalytic activities, including CuO/RGO for PEC H<sub>2</sub> generation (Dubale *et al.*, 2014), GO/g-C<sub>3</sub>N<sub>4</sub> (Xiang *et al.*, 2011; Zhang *et al.*, 2011; Babu *et al.*, 2015) for , Fe<sub>2</sub>O<sub>3</sub>/RGO (Tamirat *et al.*,

2015). Copper nanoparticle deposited on RGO have been investigated for various application including photocatalytic hydrogen production (Zhang *et al.*, 2018) and biomedical purpose (Jia *et al.*, 2015). In all these reports RGO is used as a support and electron collector and not as a light absorber. However, Cu nanoparticle decorated over the surface of semiconducting RGO as a light absorber have not been investigated for its photocatalytic organic dye degradation activity, except a report on photosensitized on  $\text{Cu}^{2+}/\text{Cu}^+$  mediated degradation of dyes on RGO (Xiong *et al.*, 2011). Here, we deposited Cu nanoparticle on RGO sheet by insitu photoreduction method. The Cu/RGO nanocomposite photocatalyst material is characterized and its photodegradation activity towards model organic dye was investigated.

## MATERIALS AND METHODS

### Synthesis of graphene oxide and reduced graphene oxide

GO were produced from pristine graphite powder (>99.8%, Alfa Aesar) using a modified Hummer's method (Hummers *et al.*, 1958). In brief, 2.0 g of graphite powder and 1.0 g of  $\text{NaNO}_3$ , and  $\text{KMnO}_4$  were maintained at temperatures below 20 °C while stirring. After removal from the ice bath, the mixture stirring was maintained for 30 min at 35 °C. Then, the solution was put in an oil bath and 92 mL of distilled water was slowly added, while the temperature of the solution was raised to 98 °C and maintained for 15 min. The reaction was terminated by adding 160 mL of distilled water followed by 17 mL of aqueous  $\text{H}_2\text{O}_2$  (30%). The product was then washed twice with 5% HCl, the resulting graphene oxide powder was collected by drying at 60 °C in an oven for 24 hr.

### Synthesis of Cu/Reduced graphene oxide nanocomposite

50 mL of different concentrations of  $\text{CuCl}_2$  aqueous solutions with 5% methanol (1.0 mM, 5.0 mM, 15 mM and 50 mM) were mixed with 5 mg of RGO powder and stirred for 30 min for the adsorption of  $\text{Cu}^{2+}$  onto the surface. Finally, the mixture was irradiated with UV light for 2.5 hr for the photoreduction of  $\text{Cu}^{2+}$  on RGO surface. The as-prepared Cu/RGO samples were rinsed with DI water and dried in an oven for further characterization and analysis.

## Characterization

X-ray diffraction measurements were performed on a D2 phaser XRD-300W diffractometer equipped with a Cu K source operating at 30 kV and 10 mA with scan range of 10–80° at a rate of 3° per min. UV-Vis absorption spectra were obtained using Cary 600 UV-Vis spectrophotometer. FTIR spectra were recorded on solid samples by making a pellet with KBr.

## Photocatalytic activity

Photocatalytic experiments were carried out by photodegrading MB dye with 100 W household light bulb and measuring the concentration change with time using UV-Vis spectroscopy. The solution of MB (pH~7) without GO was left in a dark place for 30 min followed by light irradiation. In a typical experiment, 20 mg of GO was added into a 100 mL 40 ppm MB solution. Before illumination, the suspensions were continuously stirred at dark place for 40 min to reach an adsorption-desorption equilibrium. Then, the suspensions were exposed to visible light irradiation for another 1.5 hr and samples were taken at regular time intervals for dye concentration determination. Photodegradation was also performed on RGO and Cu/RGO photocatalyst materials. The degradation efficiency was determined by using the equation shown below:

$$\begin{aligned} \text{Photodegradation efficiency (\%)} &= [(C_0 - C_t) / C_0] * 100\% & (1) \\ &= [(A_0 - A_t) / A_0] * 100\% \end{aligned}$$

Where  $C_0$  is the initial concentration of MB,  $C_t$  is the concentration of MB at time,  $t$  and  $A_0$  is the initial absorbance of MB,  $A_t$  is the absorbance after time  $t$  photo irradiation.

## RESULTS AND DISCUSSION

### UV-Visible Spectroscopy studies

The UV-visible absorption spectra of GO, RGO and Cu/RGO nanocomposite synthesized with deposition of 1, 5, 15 and 50 mM  $\text{CuCl}_2$  solutions are shown in Figure 1a. Based on the UV-visible absorption spectra, the absorption peaks of GO at 229 nm and 296 nm are due to the  $\pi - \pi^*$  transition of the aromatic C-C bond and the  $n - \pi^*$  transition of the C =

O bond, respectively (Kumar *et al.*, 2013; Rabchinskii *et al.*, 2018). After the reduction treatment, obvious absorption peaks were found between 232–234 nm. It is well known that the red shift in the UV-visible absorption spectra is mainly due to the restoration of electronic conjugation upon the UV irradiation (Yan *et al.*, 2009). The restoration of the  $sp^2$  hybridization carbon atoms increases the electron concentration. The UV-Visible absorption spectra of Cu nanoparticle decorated RGO showed new peaks at about 620 nm due to the surface plasmon resonance effect of Cu nanoparticle (Figure 1d). The shape and the position of the peak depends on the diameter of the Cu nanoparticle (Liu *et al.*, 2015). This confirms the successful loading of Cu nanoparticle on RGO surface.

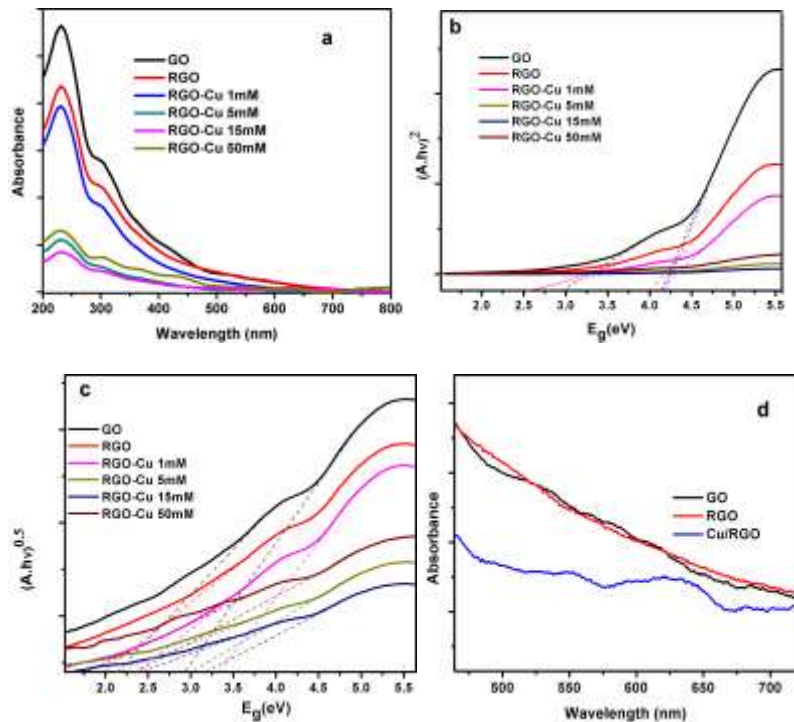


Figure 1. (a) UV-Vis absorption spectra of GO, RGO, and Cu /RGO with various concentrations of CuCl<sub>2</sub> (b) corresponding Tauc plot for direct band gap determination (c) Tauc plot for indirect band gap determination and (d) absorption spectra of GO, RGO and Cu/RGO.

Figure 1b & c show the square and square root of the absorption energy ( $Ah\nu$ , where  $A$  is the absorbance) against photon energy ( $h\nu$ ) to determine the direct and indirect optical band gap energies, respectively. Because GO comprises graphene molecules of various reduction levels, the tauc plots do not show a sharp absorption edge for a precise band gap but shows a range in band gap. From approximate linear extrapolation of the plot as shown in Figure 1b & c, the direct band gap and indirect band gap correlates to 2.97, 2.62, 3.30, 3.16, 3.20, 3.05 eV and 2.20, 1.98, 2.42, 2.35, 2.21, and 2.37eV for GO, RGO, RGO-Cu 1 mM, RGO-Cu 5mM, RGO-Cu 15 mM and RGO-Cu 50 mM specimens, respectively. Generally, the band gap of RGO is lower than that of GO, implying the photoreduction of oxygen containing functional groups on the surface of GO sheets. The gap nature of copper nanoparticle decorated reduced graphene oxide also gradually changes with increasing concentration of copper ion precursor solution. The band gap of Cu decorated RGO is a little higher than the pure RGO. It might be due to the self-oxidation RGO by photogenerated holes while the photoelectron is used for Cu ion reduction.

### FTIR analysis

The FTIR analysis of GO, RGO and Cu/RGO nanocomposite is shown in Figure 2. GO showed broad absorption peak observed at  $\sim 3414\text{ cm}^{-1}$  corresponding to O-H stretching vibration which could indicate the existence of adsorbed water molecules in addition to carboxy and hydroxy O-H groups in GO. The peak at  $1619\text{ cm}^{-1}$ ,  $1730\text{ cm}^{-1}$ ,  $1398\text{ cm}^{-1}$ ,  $1210$  and  $1046\text{ cm}^{-1}$  corresponds to vibrational stretching of unoxidized C=C aromatic ring, carboxylic (kenotic species) of C=O stretching, C-OH of hydroxyl group, and C-O stretching bond of epoxy group respectively (Choi *et al.*, 2010). After reduction the characteristic absorption of oxygen containing groups are relatively weakened in the case of RGO. There is an obvious decrease in the intensities of OH stretching vibration ( $3414\text{ cm}^{-1}$ ), C=O ( $1730\text{ cm}^{-1}$ ), C- OH ( $1398\text{ cm}^{-1}$ ) and C- O ( $1210\text{ cm}^{-1}$  and  $1046\text{ cm}^{-1}$ ) vibration peaks in RGO compared to those in GO, indicating that UV-assisted photocatalytic reduction is an effective method to remove oxygen-containing groups of GO. The presence of extensive OH peaks after reduction is due to the presence of adsorbed water molecules. In the case of Cu/RGO, the peak intensities for oxygen containing function groups are increased again. This could be explained as follows. During the photoreduction of copper ion on the surface of RGO, the photogenerated holes from the RGO could self-oxidize the RGO and hence oxygen

containing functional groups could be enhanced again. Even though methanol was used as a hole scavenger during copper ion photoreduction, a competitive reaction of the hole with methanol and RGO could lead to a certain extent of self-oxidation.

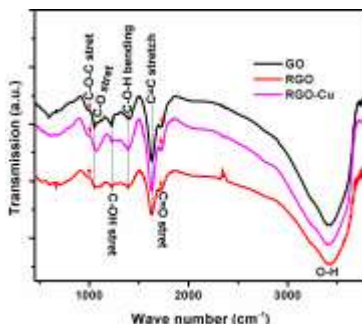


Figure 2. FTIR spectra of GO, RGO and Cu/RGO

### XRD analysis

The XRD pattern of the GO in Figure 3 shows a diffraction peak at  $11.3^\circ$  confirming the formation of an exfoliated GO and a small graphitic peak from trace amounts of unoxidized graphite. The interlayer distance of GO is higher than the precursor graphite due to the incorporated oxygen containing functional groups including hydroxyl, epoxy and carboxyl groups, allowing water molecules to intercalate between the layers. The peak shift to higher angle in RGO ( $2\theta=12^\circ$ ) shows the decrease in interlayer distance due to removal of some oxygen functionalities. The peak at about  $26^\circ$  in GO, RGO, and Cu/RGO represents trace unoxidized graphite. The lower angle shift in case of Cu/RGO is due to the increase in inter-layer spacing as a result of the self-oxidation of RGO during the photoreduction of copper ion, in agreement with the FTIR results. This is in agreement with the large optical bandgap from UV-Vis and increased oxygen functionalities from the FTIR spectra of Cu/RGO. In addition the diffraction peak at about  $42.8^\circ$  is due to the Cu nanoparticle deposited on RGO surface. The appearance of this diffraction peak in Cu/RGO nanocomposite which was absent in GO and RGO ascertains the formation of Cu nano particle by in-situ photocatalytic reduction method. The size Cu nanoparticle prepared using photoreduction of 50 mM  $\text{CuCl}_2$  solution for 2.5 hr was determined from Scherer equation (Equation 2).

$$D = K * \lambda / \beta \cos \theta \quad (2)$$

Where D is the interlayer distance,  $\lambda$  is the wavelength of the X-rays = 0.15406 nm,  $\beta$  is the peak width of half-maximum of an XRD, K is constant=0.94 and  $\theta$  is the Bragg diffraction angle. The crystalline particle size of Cu nanoparticle was found to be about 12.21 nm. The size of the particle is dependent on the concentration of  $\text{CuCl}_2$  solution used and the time of photo irradiation, where size increases with increase in concentration and time of photoreduction.

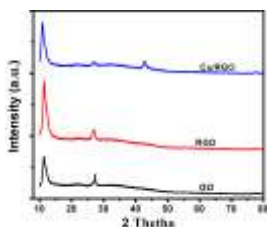


Figure 3. X-ray diffraction patterns of GO, RGO and Cu/RGO nanocomposite

### Photocatalytic activity

The photocatalytic activity of GO, RGO and Cu/RGO nanocomposite were evaluated by monitoring the concentration change of MB dye as a function of light irradiation time using UV-Vis spectroscopy. The dye has an intense absorption peak at 664 nm and the absorbance of the initial dye concentration was determined. The absorbance of the dye decreased with increasing time of light irradiation as shown in Figure 4a. The first 10 min of photocatalytic degradation of MB was dramatic and showed similar trends for GO, RGO and Cu/RGO. Under UV-Vis light irradiation GO, RGO, and Cu/RGO showed 63%, 68% and 94% photodegradation efficiency after 50 min, respectively. Photocatalytic degradation efficiency is summarized in Table 1.

Table 1. Photocatalytic degradation efficiency of MB by GO, RGO and Cu/RGO.

Photocatalyst	Concentration of MB (ppm)	Amount of photocatalyst (mg)	Degradation efficiency after 50 min (%)
GO	40	20	63
RGO	40	20	68
Cu/RGO	40	20	94

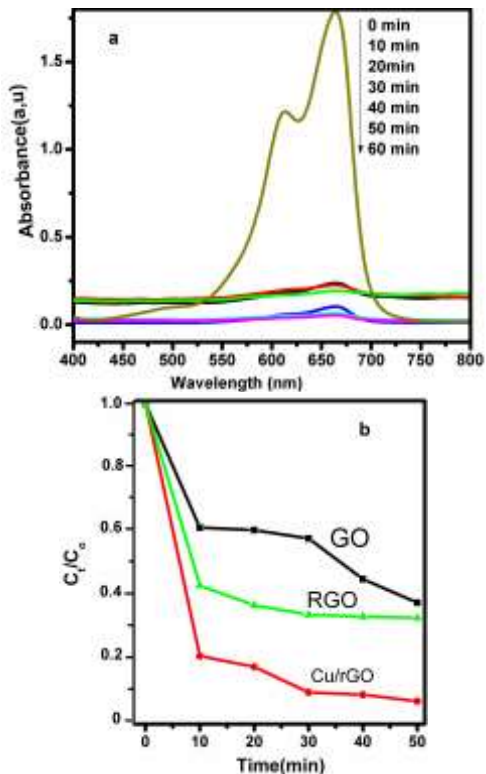


Figure 4. Time-dependent absorption spectra of MB solution during light irradiation in the presence of Cu/RGO (a) and rate of MB dye photodegradation with GO, RGO and Cu/RGO nanocomposite (b)

It is clear from Figure 4(b) Cu/RGO nanocomposite showed the highest photocatalytic activity compared to that of GO and RGO only. The lower photocatalytic activity GO could be due to the larger band gap that would limit its absorption in the visible region. The major light absorber is the RGO and the photogenerated electrons and holes can be efficiently separated in the presence of Cu nanoparticle. In addition, the high photocatalytic performance of Cu/RGO nanocomposite is due to the catalytic effect of Cu. The Cu nanoparticle is a good photoelectron acceptor that traps the photoelectron and reduces the recombination rate of photoelectron-hole pairs. This makes an efficient hole transfer to the surface of RGO for dye degradation. Later, the photoelectron can also react with the dissolved

oxygen in the solution to form superoxides that can oxidize the dye (Wang *et al.*, 2012). Hence the presence of Cu nanoparticle plays a vital role in as an electron trap which enhances the charge separation efficiency and hence leading to better dye degradation rate relative to pristine GO and RGO.

## CONCLUSIONS

In summary, RGO and Cu/RGO nanocomposites were successfully synthesized by simple insitu photoreduction method. Optical absorption demonstrated that the band gap energy of GO decreases with the photoreduction. The potential of GO, RGO and Cu/RGO nanocomposites as a photocatalyst was evaluated by photodegradation of MB under UV-light irradiation. Based on our studies, Cu/RGO nanocomposites showed higher photocatalytic activity than GO and RGO. The photocatalytic degradation efficiency of GO, RGO and Cu/RGO nanocomposites were 63%, 68% and 94% respectively under light irradiation at pH~7 in 50 min. We believe that our finding would be widely applicable to the grapheme oxide-based composites with metal or metal oxide nanoparticles to develop a cost-effective technique for environmental protection.

## REFERENCES

- Akbal, F. (2005). Photocatalytic degradation of organic dyes in the presence of titanium dioxide under UV and solar light: Effect of operational parameters. *Environmental Progress* **24**(3): 317-322. doi: 10.1002/ep.10092.
- Babu, S.G., Vinoth, R., Narayana, P.S., Bahnemann, D and Neppolian, B. (2015). Reduced graphene oxide wrapped Cu<sub>2</sub>O supported on C<sub>3</sub>N<sub>4</sub>: An efficient visible light responsive semiconductor photocatalyst. *APL Materials* **3**(10):104415. doi: 10.1063/1.4928286
- Barka, N., Qourzal, S., Assabbane, A., Nounah, A and Ait-Ichou, Y. (2010). Photocatalytic degradation of an azo reactive dye, Reactive Yellow 84, in water using an industrial titanium dioxide coated media. *Arabian Journal of Chemistry* **3**(4): 279-283. doi: <https://doi.org/10.1016/j.arabjc.2010.06.016>
- Carcel, R.A., Andronic, L and Duta, A. (2011). Photocatalytic degradation of methylorange using TiO<sub>2</sub>, WO<sub>3</sub> and mixed thin films under controlled pH and H<sub>2</sub>O<sub>2</sub>. *Journal of Nanoscience and Nanotechnology* **11**(10): 9095-9101. doi: 10.1166/jnn.2011.4283

- Choi, E.-Y., Han, T.H., Hong, J., Kim, J.E., Lee, S.H., Kim, H.W and Kim, S.O. (2010). Noncovalent functionalization of graphene with end-functional polymers. *Journal of Materials Chemistry* **20**(10): 1907-1912. doi: 10.1039/B919074K
- da Silva, C.G and Faria, J.L.S. (2003). Photochemical and photocatalytic degradation of an azo dye in aqueous solution by UV irradiation. *Journal of Photochemistry and Photobiology A: Chemistry* **155**(1): 133-143. doi: [https://doi.org/10.1016/S1010-6030\(02\)00374-X](https://doi.org/10.1016/S1010-6030(02)00374-X)
- Dubale, A.A., Su, W.N., Tamirat, A.G., Pan, C.J., Aragaw, B.A., Chen, H.M., Chen, C.H and Hwang, B.J. (2014). The synergetic effect of graphene on Cu<math>^{2+}</math>/O nanowire arrays as a highly efficient hydrogen evolution photocathode in water splitting. *Journal of Materials Chemistry A* **2**(43): 18383-18397. doi: 10.1039/c4ta03464c
- Hsu, H.-C., Shown, I., Wei, H.-Y., Chang, Y.-C., Du, H.-Y., Lin, Y.-G., Tseng, C.-A., Wang, C.-H., Chen, L.-C., Lin, Y.-C and Chen, K.-H. (2013). Graphene oxide as a promising photocatalyst for CO<sub>2</sub> to methanol conversion. *Nanoscale* **5**(1): 262-268. doi: 10.1039/C2NR31718D
- Hummers, W.S and Offeman, R.E. (1958). Preparation of graphitic oxide. *Journal of the American Chemical Society* **80**(6): 1339-1339. doi: 10.1021/ja01539a017
- Jia, Z., Chen, T., Wang, J., Ni, J., Li, H and Shao, X. (2015). Synthesis, characterization and tribological properties of Cu/reduced graphene oxide composites. *Tribology International* **88**: 17-24. doi: <https://doi.org/10.1016/j.triboint.2015.02.028>
- Jiang, X., Nisar, J., Pathak, B., Zhao, J and Ahuja, R. (2013). Graphene oxide as a chemically tunable 2-D material for visible-light photocatalyst applications. *Journal of Catalysis* **299**: 204-209. doi: <https://doi.org/10.1016/j.jcat.2012.12.022>
- Kumar, P., Bansiwala, A., Labhsetwar, N and Jain, S.L. (2015). Visible light assisted photocatalytic reduction of CO<sub>2</sub> using a graphene oxide supported heteroleptic ruthenium complex. *Green Chemistry* **17**(3): 1605-1609. doi: 10.1039/C4GC01400F
- Kumar, P.V., Bardhan, N.M., Tongay, S., Wu, J., Belcher, A.M and Grossman, J.C. (2013). Scalable enhancement of graphene oxide properties by thermally driven phase transformation. *Nature Chemistry* **6**: 151. doi: 10.1038/nchem.1820
- Liu, H., Wang, T and Zeng, H. (2015). CuNPs for efficient photocatalytic hydrogen evolution. *Particle & Particle Systems Characterization* **32**(9):869-873. doi: 10.1002/ppsc.201500059

- Liu, Y., Zeng, X., Hu, X., Hu, J and Zhang, X. (2019). Two-dimensional nano-materials for photocatalytic water disinfection: recent progress and future challenges. *Journal of Chemical Technology & Biotechnology* **94**(1):22-37. doi: 10.1002/jctb.5779
- Mahmoodi, N.M., Keshavarzi, S and Ghezelbash, M. (2017). Synthesis of nanoparticle and modelling of its photocatalytic dye degradation ability from colored wastewater. *Journal of Environmental Chemical Engineering* **5**(4): 3684-3689. doi: <https://doi.org/10.1016/j.jece.2017.07.010>
- Nezamzadeh-Ejehieh, A and Hushmandrad, S. (2010). Solar photodecolorization of methylene blue by CuO/X zeolite as a heterogeneous catalyst. *Applied Catalysis A: General* **388**(1): 149-159. doi: <https://doi.org/10.1016/j.apcata.2010.08.042>
- Nezamzadeh-Ejehieh, A and Karimi-Shamsabadi, M. (2013). Decolorization of a binary azo dyes mixture using CuO incorporated nanozeolite-X as a heterogeneous catalyst and solar irradiation. *Chemical Engineering Journal* **228**: 631-641. doi: <https://doi.org/10.1016/j.cej.2013.05.035>
- Nezamzadeh-Ejehieh, A and Karimi-Shamsabadi, M. (2014). Comparison of photocatalytic efficiency of supported CuO onto micro and nano particles of zeolite X in photodecolorization of Methylene blue and Methyl orange aqueous mixture. *Applied Catalysis A: General* **477**: 83-92. doi: <https://doi.org/10.1016/j.apcata.2014.02.031>
- Rabchinskii, M.K., Dideikin, A.T., Kirilenko, D.A., Baidakova, M.V., Shnitov, V.V., Roth, F., Konyakhin, S.V., Besedina, N.A., Pavlov, S.I., Kuricyn, R.A., Lebedeva, N.M., Brunkov, P.N and Vul', A.Y. (2018). Facile reduction of graphene oxide suspensions and films using glass wafers. *Scientific Reports* **8**(1): 14154. doi: 10.1038/s41598-018-32488-x
- Rajamanickam, D and Shanthi, M. (2016). Photocatalytic degradation of an organic pollutant by zinc oxide – solar process. *Arabian Journal of Chemistry* **9**: S1858-S1868. doi: <https://doi.org/10.1016/j.arabjc.2012.05.006>
- Sun, H., Liu, S., Zhou, G., Ang, H.M., Tadó, M.O and Wang, S. (2012). Reduced graphene oxide for catalytic oxidation of aqueous organic pollutants. *ACS Applied Materials & Interfaces* **4**(10): 5466-5471. doi: 10.1021/am301372d
- Sun, L., Du, T., Hu, C., Chen, J., Lu, J., Lu, Z and Han, H. (2017). Antibacterial activity of graphene oxide/g-C<sub>3</sub>N<sub>4</sub> composite through photocatalytic disinfection under visible light. *ACS Sustainable Chemistry & Engineering* **5**(10): 8693-8701. doi: 10.1021/acssuschemeng.7b01431

- Tamirat, A.G., Su, W.-N., Dubale, A.A., Pan, C.-J., Chen, H.-M., Ayele, D.W., Lee, J.-F and Hwang, B.-J. (2015). Efficient photoelectrochemical water splitting using three dimensional urchin-like hematite nanostructure modified with reduced graphene oxide. *Journal of Power Sources* **287**: 119-128. doi: <https://doi.org/10.1016/j.jpowsour.2015.04.042>
- Tanaka, K., Padermpole, K and Hisanaga, T. (2000). Photocatalytic degradation of commercial azo dyes. *Water Research* **34**(1): 327-333. doi: [https://doi.org/10.1016/S0043-1354\(99\)00093-7](https://doi.org/10.1016/S0043-1354(99)00093-7)
- Wang, J.L and Xu, L.J. (2012). Advanced oxidation processes for wastewater treatment: Formation of hydroxyl radical and application. *Critical Reviews in Environmental Science and Technology* **42**(3): 251-325. doi: [10.1080/10643389.2010.507698](https://doi.org/10.1080/10643389.2010.507698)
- Wei, Y., Zhu, Y and Jiang, Y. (2019). Photocatalytic self-cleaning carbon nitride nanotube intercalated reduced graphene oxide membranes for enhanced water purification. *Chemical Engineering Journal* **356**: 915-925. doi: <https://doi.org/10.1016/j.cej.2018.09.108>
- Xiang, Q., Yu, J and Jaroniec, M. (2011). Preparation and enhanced visible-light photocatalytic H<sub>2</sub>-production activity of graphene/C<sub>3</sub>N<sub>4</sub> composites. *The Journal of Physical Chemistry C* **115**(15): 7355-7363. doi: [10.1021/jp200953k](https://doi.org/10.1021/jp200953k)
- Xiong, Z., Zhang, L.L and Zhao, X.S. (2011). Visible-light-induced dye degradation over copper-modified reduced graphene oxide. *Chemistry – A European Journal* **17**(8): 2428-2434. doi: [10.1002/chem.201002906](https://doi.org/10.1002/chem.201002906)
- Yan, J.-A., Xian, L and Chou, M.Y. (2009). Structural and electronic properties of oxidized graphene. *Physical Review Letters* **103**(8): 086802. doi: [10.1103/PhysRevLett.103.086802](https://doi.org/10.1103/PhysRevLett.103.086802)
- Yeh, T.-F., Chan, F.-F., Hsieh, C.-T and Teng, H. (2011). Graphite oxide with different oxygenated levels for hydrogen and oxygen production from water under illumination: The band positions of graphite oxide. *The Journal of Physical Chemistry C* **115**(45): 22587-22597. doi: [10.1021/jp204856c](https://doi.org/10.1021/jp204856c)
- Yeh, T.-F., Syu, J.-M., Cheng, C., Chang, T.-H and Teng, H. (2010). Graphite oxide as a photocatalyst for hydrogen production from water. *Advanced Functional Materials* **20**(14): 2255-2262. doi: [10.1002/adfm.201000274](https://doi.org/10.1002/adfm.201000274)
- Zang, Z., Hossain, M.F and Takahashi, T. (2010). Self-assembled hematite ( $\alpha$ -Fe<sub>2</sub>O<sub>3</sub>) nanotube arrays for photoelectrocatalytic degradation of azo dye under

- simulated solar light irradiation. *Applied Catalysis B: Environmental* **95**(3): 423-429. doi: <https://doi.org/10.1016/j.apcatb.2010.01.022>
- Zhang, L.L., Xiong, Z and Zhao, X.S. (2010). Pillaring chemically exfoliated graphene oxide with carbon nanotubes for photocatalytic degradation of dyes under visible light irradiation. *ACS Nano* **4**(11): 7030-7036. doi: 10.1021/nn102308r
- Zhang, P., Song, T., Wang, T and Zeng, H. (2018). Plasmonic Cu nanoparticle on reduced graphene oxide nanosheet support: An efficient photocatalyst for improvement of near-infrared photocatalytic H<sub>2</sub> evolution. *Applied Catalysis B: Environmental* **225**: 172-179. doi: <https://doi.org/10.1016/j.apcatb.2017.11.076>
- Zhang, Y., Mori, T., Niu, L and Ye, J. (2011). Non-covalent doping of graphitic carbon nitride polymer with graphene: controlled electronic structure and enhanced optoelectronic conversion. *Energy & Environmental Science* **4**(11): 4517-4521. doi: 10.1039/C1EE01400E

